

## Filtered-OFDM for 5G Wireless Communication Narrow-band IoT Systems

Ashutosh Pandey\*\* and Deepak Sharma\*

\*\*Research scholar, Assistant Professor\*

Department of Electronics and Communications

<sup>1,3</sup>Jaypee University of Engineering and Technology,

A. B. Road, Guna, India,

---

**Abstract:** The emerging Internet of Things (IoT) technology, devices will make the next generation 5G systems enable to support in diversify demands with greater efficiency in social, technical and economic dimensions. The era of 5G communication has empowered us with higher data transmission rate, user-friendly environment and better resource utilization capabilities equipped within it. In order to achieve these 5G technology attribute, we need to have small data packets and narrow bands with low power consumption. Hence, narrow-band IoT (NB-IoT) devices may play very vital and important role to fulfil these goals. The standard or conventional Orthogonal Frequency Division Multiplexing (OFDM) suffers with high peak to average ratio (PAPR), high side lobes causing undesired spectral leakage and channel interference. However, spectrally-localized waveform is achieved by using filtered orthogonal frequency division multiplexing (F-OFDM) by setting the filter length larger than the cyclic prefix (CP) length of an OFDM system. In proposed F-OFDM waveform, we can achieve localized frequency spectrum for narrow bandwidths and maintaining the inter-symbol interference/inter-carrier interference (ISI/ICI), BER and PAPR within an acceptable range. The key contribution in this paper is the filtered OFDM (F-OFDM) system performance has been analysed for narrow band IoT with Cyclic Prefix OFDM (CP-OFDM). Analysing the results, it is found that the F-OFDM system has achieved better PAPR than conventional OFDM system with least Bit Error Rate (BER) in the range of 20-40 dB of SNR for 5G supporting IoT systems.

**Keywords:** Internet of thing (IoT), Narrow band, Filtered-Orthogonal Frequency Division Multiplexing (F-OFDM), 5G communication, Peak to Average Power Ratio (PAPR), Bit Error Rate (BER), Signal to Noise Ratio (SNR)

---

Date of Submission: 02-06-2020

Date of Acceptance: 17-06-2020

---

### I. Introduction

In recent years, the growing demand for higher data rates has boosted an interest in new emerging technologies that might be used to meet these new requirements like higher transmission rate, user-friendly experience, resource utilization, etc [1]. In the current scenario, the expectation for 5G and everything it promises to offer is great extent[2], [3]. In order to efficiently support the diverse requirements of 5G and spectrum efficient, one of the fundamental and key challenges over the previous systems, e.g., orthogonal frequency division multiplexing (OFDM) based long term evolution (LTE) [4], is the new waveform design to enable the multi-service signal multiplexing and isolation [5]. In spite of traditional advantages of the OFDM systems, such as ease of implementation of channel estimation/ equalization techniques, there are vital important features that the filtered-OFDM must carry to maintain the overall design requirements of 5G systems for IoT devices like: low out of band emission (OoBE) i.e. less spectral leakage and relief in synchronization requirements [5], [6].

In addition, this feature spectrum efficient transmission provides a solid foundation for moving into and enabling multiple types of services with different optimal frame structures of communication systems co-existing in one baseband with almost negligible interference [6], [7]. In addition, the relaxed synchronization can lead to simplified hardware/algorithm design and transceiver processing [8]. Whereas, the low complexity low cost MTC devices may not have sophisticated RF hardware and simple baseband synchronization algorithms [9], [10]. Asynchronous transmission adopted in 5G for uplink transmission to save the synchronization signaling overhead during the LTE uplink transmission in mMTC systems. The proposed f-OFDM, an asynchronous filtered orthogonal frequency division multiple access (f-OFDMA) scheme is introduced, which uses the spectrum shaping filter at each transmitter for side lobe leakage elimination and a

bank of filters at the receiver for inter-user interference rejection, inter channel interference (ISI) and adjacent channel interference (ACI).

There are many waveforms have been proposed by the researchers to meet these design criterion and requirements, such as filterbank multi-carrier (FBMC) generalized frequency division multiplexing (GFDM) [11], [12], universal filtered multi-carrier (UFMC) [13], filtered orthogonal frequency division multiplexing (F-OFDM) [6] and their variants [14], [15]. The FBMC system offers the best OoBE and time-frequency localization properties but in channel estimation and during equalization MIMO-antennas system becomes more complex than OFDM due to the intrinsic interference. Recently, the Chen et. al.[16] proposed a low complexity one-tap channel equalization algorithm with additional cyclic prefix (CP) insertion to the original FBMC system [16]. The blockwise Alamouti schemes for FBMC systems has been proposed with complex orthogonality for low to- middle frequency selectivity channels, [17]. Like FBMC, GFDM is also a per-subcarrier filtered and block-based-processing system that may not be applicable to the latency sensitive services (e.g., vehicle to vehicle). Both UFMC system and F-OFDM are per subband filtered and symbol-based-processing waveforms. One of the major differences between them is that UFMC uses short filter and the filter tail does not extend to the next symbol at the transmitter. Whereas, F-OFDM normally adopts much longer filter. However, the filter tails extend to the adjacent symbols to keep the system overhead the same as the CP OFDM system. This overlapping may make the system incur more inter-symbol-interference (ISI) and inter-carrier-interference (ICI) than the UFMC system in a scenario wherein a subband occupies small percentage of the whole bandwidth. However, the longer filter and soft overlapping among adjacent symbols in F-OFDM render the system much more robust to the adjacent-carrier-interference (ACI) and the multiple-access-interference (MAI) in the asynchronous systems (for uplink). Since this is one of the main targets and a challenging communication scenarios for 5G. in this paper will be focused on the F-OFDM system only. However, the basic idea could be extended to other waveforms such as UFMC. F-OFDM uses filter with length up to half of the symbol duration for good frequency localization. This design criterion may make the system vulnerable to ISI and ICI.

The aim of this article is to demonstrate the results obtained through simulations comparing OFDM techniques and f-OFDM for IoT devices with 5G is one of the potential modulations of this new system. In OFDM systems, when signals are transmitted at adjacent frequencies (or channels), it is possible to observe that the signals leak into the adjacent channels. Therefore, by employing f-OFDM, the interference generated between the signals is expected to be smaller, decreasing the bit error rate, and increasing the spectral efficiency, as signals can better coexist. In addition to the tradeoff between overhead and performance, the tradeoff between complexity and performance is another important consideration in the system design. In the original F-OFDM system with small subband bandwidth (e.g., 12 subcarriers as a subband) to support multiple users/services, each subband may require an independent Discrete Fourier Transform (DFT) or fast Fourier transform (FFT) operation. The complexity issue is also a major challenge for low cost low complexity devices (e.g., internet of things (IoT) devices), where narrow band IoT has been proposed as a promising solution for 5G system to balance the performance and system implementation complexity [3], [10], [16]. However, with the original F-OFDM system, the FFT size and sampling rate should be kept as high as the normal user devices to secure the orthogonality among subbands, which may be against the design principles for low complexity low cost devices.

This article is organised in four major sections. The first segment discuss about the introduction about the introduction of 5G technology, IoT systems using F-OFDM system. The second segment describe the proposed Filtered OFDM system for IoT system model and their mathematical analysis is presented. The third part demonstrate the outcome received from the proposed model and their results have been discussed briefly. The fourth segment conclude the entire article and its scope of future.

## **II. Proposed System Model**

In this section, we present a proposed filtered- OFDM (f-OFDM) multi-rate system model, its implementation and the employed modulation and demodulation methods and the detection algorithms also evaluated and analysed at the receiving side of the system. The communication model is analyzed for transmission and reception in two scenarios, in the first one, each transmitted signal goes through conventional OFDM modulation and the in the second scenario, F-OFDM system is employed with QAM. The F- OFDM is one of the emerging method for 5G waveforms to optimizes the operation of OFDM by reducing the Out of Band Emission OoBE frequently also known as spectral leakage. The F-OFDM model is based on the transmission three sets of signals at three adjacent frequencies (i.e.,  $f_{c1}$ ,  $f_{c2}$ ,  $f_{c3}$ ), as showed in Fig. 1, but can be implemented with  $K$  no. of signals for different  $K$  no. of different set of IoT devices. In this perspective, the effect of filtering on the OFDM signals is evaluated and analysed for different set of IoT devices. A normal CP-OFDM process is implemented on per sub-band basis as shown in Figure-1. Then a sub-band filter is followed with the output data length being altered due to the filter tails. However, the tail of the current symbol overlaps with the next symbol and therefore it does not create an extra overhead on processing. The sub-band filter plays the role of isolating the interference from the adjacent sub-bands and hence consequently it reduces the OoBE or

spectral leakage. At the receiver side, as shown in Figure-2, an optional matched filter is used followed by CP removal and DFT or FFT processing.

The uplink transmission system uses reverse procedure with an optional DFT spreading on the modulated symbols for peak-to-average-power-ratio (PAPR) reduction. However, to focus on the interference analysis and its cancelation algorithms, we will consider the PAPR reduction algorithms in this research article.

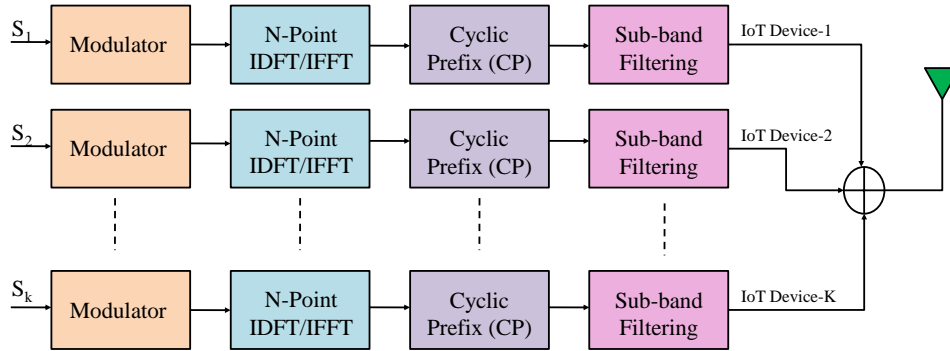


Figure-1 Multirate based Filtered-OFDM Transmitter Block

Let us consider an F-OFDM system contains  $N$  subcarriers that are divided into  $K$  sub-bands with each subband transmitting  $M$  contiguous subcarriers, i.e.,  $N = M \cdot K^{-1}$ .

The transmitted symbols in the vector form can be given by:

$$s = [s_1; s_2; \dots; s_K] \tag{1}$$

Where

$$s_k = [s_k(1); s_k(2); \dots; s_k(M)]^T \tag{2}$$

is the signal transmitted in the  $k$ -th subband. We assume  $|s_k(i)|^2 = \rho_s^2$ , for  $i = 0, 1, 2 \dots N - 1$ . Generally, multiple sub-bands can be assigned to one user or for multi users [5].

In order to simplify the derivations and with no loss condition that each user has been assigned a single sub-band, i.e., the  $k$ -th subband is allocated to the  $k$ -th user.

The transmitted signal before sub-band filtering for the  $k$ -th sub-band can be given by  $R D_k E_k s_k$ , where  $R$  is the matrix form that indicate the cyclic prefix insertion operation, so  $R = [0_{LCP \times (N \times LCP)}; I_{LCP}; I_N]$ , with  $I_{LCP}$  being the CP length and  $L_{SYM} = N + LCP$  is the symbol duration in F-OFDM samples. The  $D_k$  is the  $[(k - 1)M + 1]$ -th to the  $(kM)$ -th columns of the  $N$ -point normalized inverse DFT (IDFT) matrix  $D$ . The element of  $D$  in the  $i$ -th row and  $n$ -th column is given by  $D(i; n) = \frac{1}{\sqrt{N}} e^{-j2\pi i n / N}$

Let us assume that the  $k$ -th subband filter impulse response is

$$a_k = [a_k(1); a_k(2); \dots; a_k(L_F)] \tag{3}$$

with  $L_F$  being the filter length. In addition, we assume all subbands use the same prototype filter for our analysis otherwise system has an adaptability of applying with different filter length and type as per the requirement of IoT devices. Here, the energy of  $a_k$  is normalized to unity, by considering  $\sum_{l=1}^{L_F} |a_k(l)|^2 = 1$ . In order to express the transmitter system model into the matrix form, let us define an  $[(L_{SYM} + L_F) \times L_{SYM}]$  dimension Toeplitz matrix  $A_k$  with its first column being  $[a_k; 0_{1 \times (L_{SYM})}]^T$  and first row being  $[a_k(1); 0_{1 \times (L_{SYM})}]^T$ . The transmitted signal after sub-band filtering for the  $k$ -th sub-band as  $A_k R D_k E_k s_k$ . The number of overall samples that contains the transmitted signal is  $L_{SYM} + L_F$  due to the filter tails. After filter tail overlapping, the current symbol at the  $k$ -th sub-band will be overlapped with one previous and one next symbol 3. In this case, we can write the  $k$ -th sub-band signal before transmission as,

$$q_k = \frac{1}{\rho_k} [R_{DESk} + R_{Noise,k}] \tag{4}$$

where the first term  $R_{DESk} = A_k R D_k E_k s_k$  is the desired signal. The second term is the Noise ISI due to the filter tail overlapping with the previous and next symbol.

At the receiver side, Let us assume the channel impulse response between the transmitter and the  $k$ -th user is  $b_k = [b_k(1); b_k(2); \dots; b_k(L_{CHK})]$  where  $L_{CHK}$  is the length of the channel in F-OFDM samples. Due to the consideration of different user and for them different IoT devices the different taps of the channel are uncorrelated, hence,  $\varepsilon\{b_k(i)b_k^*(l)\} = 0$  if  $i \neq l$  and  $\varepsilon\{b_k(i)b_k^*(l)\} = R_k$  if  $i = l$ .

we assume the overall channel gain for the  $k$ -th user for no loss is  $\sum_{i=1}^{L_{CHK}} \varepsilon = 0 |b_k(i)|^2 = \rho_{CHK}^2$ . The samples that contains the desired signal should be selected by making the trade off between the ISI between consecutive symbols in the  $k$ -th sub-band. The channel matrix is convoluted with the transmitted signal for the detection of desired received signal.

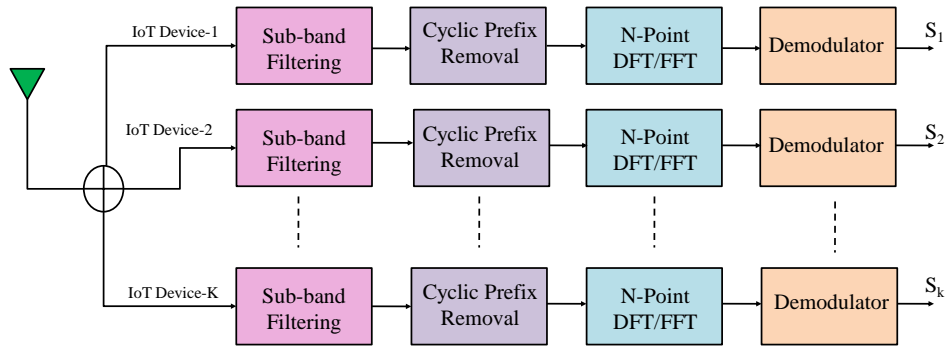


Figure-2 Multirate based Filtered-OFDM Receiver Block

The ISI was received by calculating between the consecutive symbols. The linear receiver filtering, CP removal and DFT processing is performed one by one, let us write the received signal at the  $k - th$  user as:

$$y_k = y_{DES;k} + y_{ISI;k} + y_{ACI;k} \tag{5}$$

Where  $y_{DES;k}$  is the desired received signal and the terms  $y_{ISI;k}$  is ISI received during the transmission and  $y_{ACI;k}$  is adjacent carrier interference between symbols.

### III. Results And Discussion

In this section, we present and assessment of the results regarding the two model scenarios of standard OFDM and Filtered-OFDM. The Monte-Carlo simulations is used to achieve F-OFDM and conventional OFDM systems results and derived ICI and ISI power for different sub-carrier indexes and cyclic prefix length for MR F-OFDM are also examined.

The impact of system parameters like filter length, CP length are analysed on the F-OFDM system performance and compared our simulated results in terms of the ICI power and ISI power for filtered-OFDM system

The following parameters are used for simulations in F-OFDM. The signal is modulated using 16-QAM modulation scheme with normalized power to unity. The input SNR is controlled by the additive Gaussian noise variance. The filter length and CP length are kept at 50% and 7% of a symbol duration are selected for comparison purpose respectively. The same results also achieved for standard OFDM systems for comparison along with contemporary scheme. In order to compare the simulation, The total subcarriers are split into 3 sub-bands each containing upto 14 subcarriers. The Figure-3 shows the simulated interference power for the subband. It can be seen that all of the simulated results shows the effectiveness of received signal in terms of their interchannel interference power and intersymbol interference power. In Figure-3 the ICI and ISI is also compared with contemporary scheme given by Zhang et.al. [6]. The proposed scheme is found -5dB ISI and -4.2dB ICI better than the scheme given by Zhang et.al [6]. It is very clearly depicted in Figure-3 that ISI shows larger impact on the system than ICI. However, the proposed shown better performance over the scheme given by the Zhang et.al. [6].

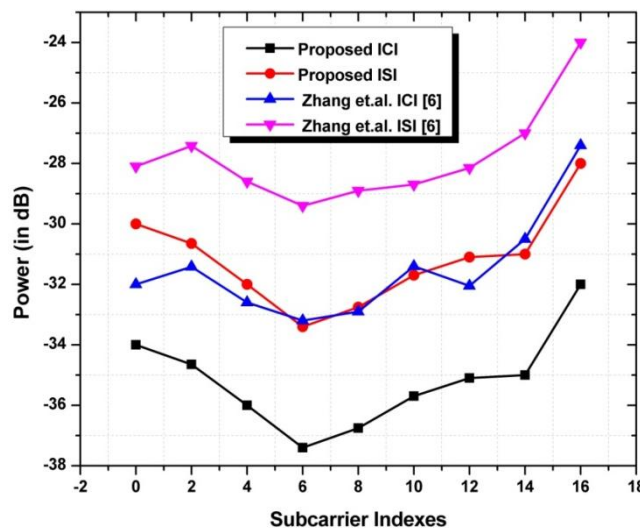


Figure-3 ICI and ISI power versus sub-carrier indexes

In order to show the relationship between the filter length and the ACI level, the simulated results for ACI versus subcarrier index with different filter lengths are shown in Figure-4.

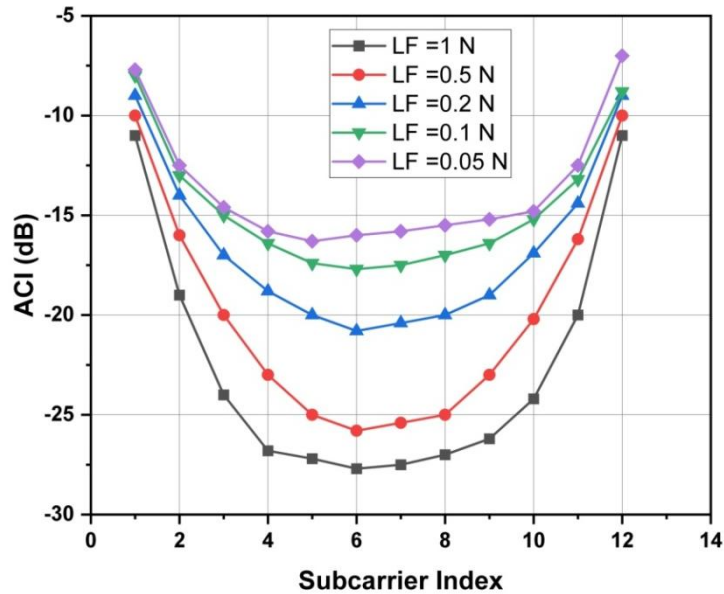


Figure-4 ACI power versus subcarrier index with different filter length

It is clearly depicted in the figure-4 that the ACI level drops monotonically when the filter length increases. The major cause of dropping ACI is longer CP creates high probability of synchronization between subbands. However, in the cases considered from  $0.05N$  to  $0.5N$  shows for the F-OFDM system can mitigate the ACI effectively as compared with the OFDM system ACI calculated at  $L_F = 1.N$ .

The affect of CP length versus ISI and ICI power are analysed for the F-OFDM system. The simulation results are shown in Figure-5 in terms of ICI and ISI at the first subcarrier of subband. It is clearly depicted that both ICI and ISI drop whenever the CP length increases upto 0.2 but beyond 0.2 to 0.4 length of cyclic prefix the ISI and ICI increases. However, ICI seems more sensitive to the change than ISI and it is almost negligible as compared to ISI but significant in comparison to the scheme proposed by Zhang et. al. [6] when the CP length is set as 7% of the symbol duration. The proposed scheme is -4dB better than interms of ICI and -10 dB better than interms of ISI power than the contemporary scheme given by Zhang et.al. [6]. However, the affect on ISI is significant but same time the affect of large CP is not very significant on ICI with large CP length.

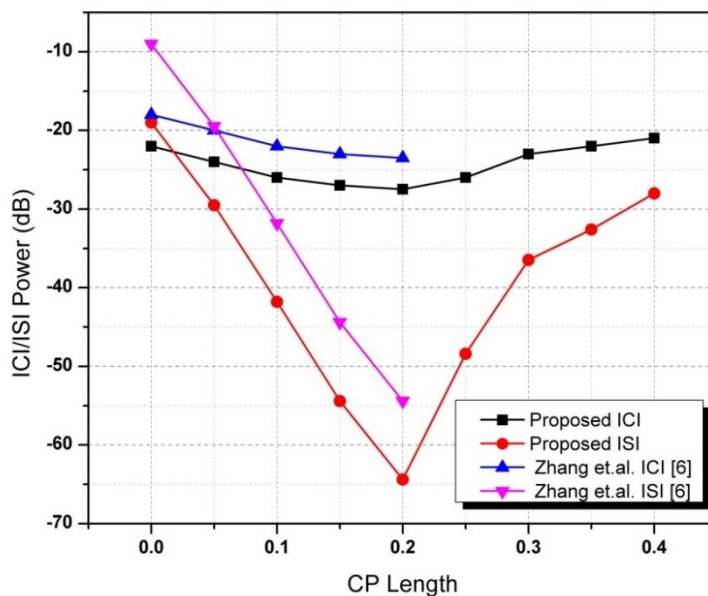


Figure-5 The ICI and ISI power at different length of cyclic prefix CP

In Figure-6, we compared the overall interference at the subcarrier for standard conventional OFDM and F-OFDM systems. It has been clearly observed that the F-OFDM offer smaller overall interference over the conventional OFDM system, thus, it expects that F-OFDM system has a potential to have better BER performance than conventional OFDM system. The proposed filtered OFDM system is also compared with the contemporary scheme of filtered-OFDM given by Zhang et.al. [6]. The proposed filtered OFDM scheme found 1.6 dB better for large cyclic prefix length. However, for smaller cyclic prefix length overall interference power is not very significant and found comparable with the scheme given by Zhang et.al.[6].

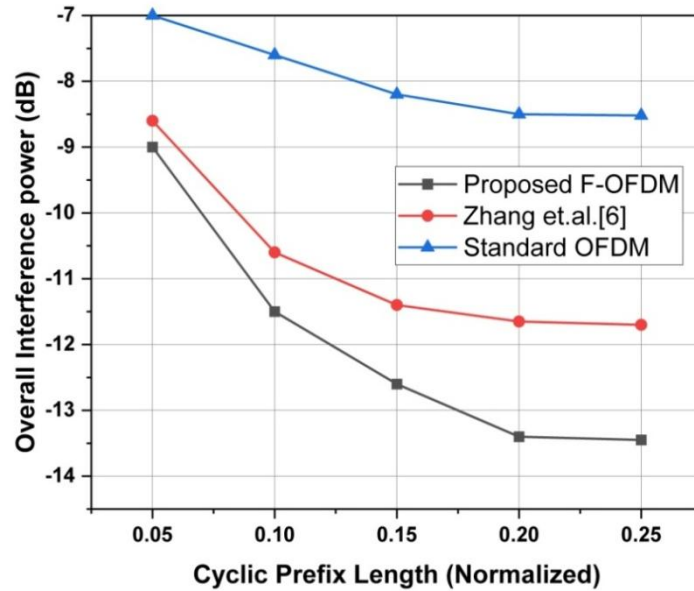


Figure-6 Overall interference power versus CP length.

In Figure-7, the performance of filtered-OFDM is investigated based on bit error rate versus signal to noise ratio (SNR).

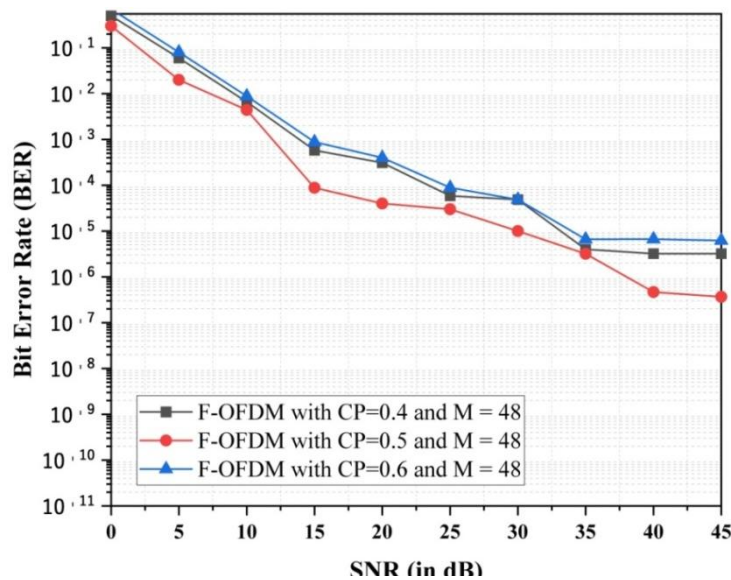
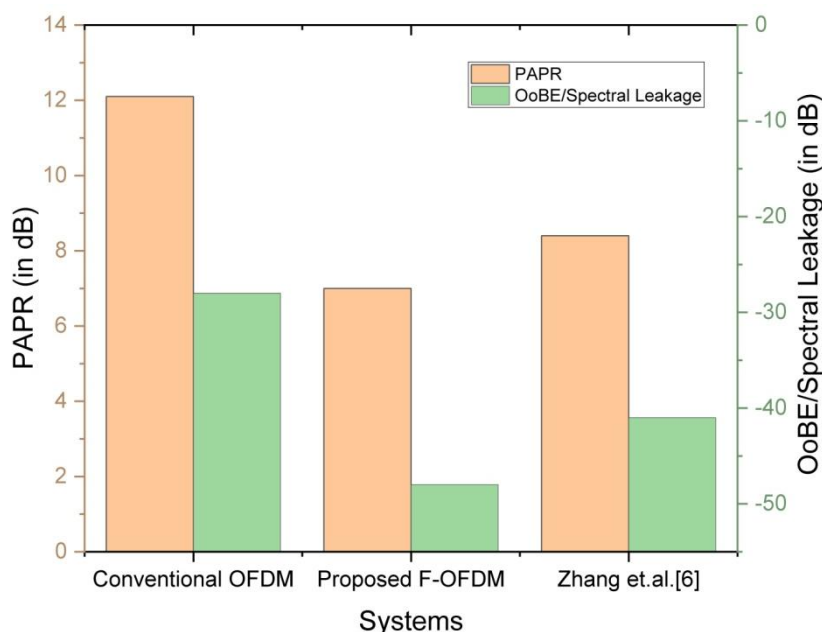


Figure-7 Bit error rate versus signal to noise ratio at different values of CP

The simulation performance of filtered OFDM system is evaluated for the different values of CP with the sub-band bandwidth  $M = 48$  and it had been observed that longer cyclic prefix length and large sub-band bandwidth provides better performance in bit error rate. In large sub band the more energy is concentrated and the leakage to the adjacent symbol become less hence the lesser bit error rate. However, the conventional OFDM system has a large BER in comparison to F-OFDM. In addition, it can be seen that the performance of F-OFDM is far better in comparison to conventional OFDM power scenario at the transmitter side is significant. It is clearly depicted in figure-7 that the BER is about  $10^{-6}$  at the SNR of 45dB.



**Figure-8** Comparison of PAPR and OoBE for the conventional OFDM, proposed F-OFDM and contemporary scheme

In Figure-8, the comparison among the conventional OFDM, proposed F-OFDM and contemporary scheme given by Zhang et.al. [6] is done and analysed based on PAPR and out of band emission (OoBE) or spectral leakage. The proposed filtered-OFDM system for IoT devices used  $7\text{ dB}$  of PAPR whereas the conventional OFDM system takes  $12.1\text{ dB}$  and the scheme given by Zhang et.al. [6] use  $8.4\text{ dB}$  of PAPR. Similarly the proposed system also indicate less spectral leakage of  $-48.1\text{ dB}$  whereas the scheme given by Zhang et.al. [6] provide  $-41.6\text{ dB}$  and conventional OFDM system has large spectral leakage among all of them with  $-28\text{ dB}$ . Hence the proposed F-OFDM system is  $6.5\text{ dB}$  superior in OoBE over the scheme given by Zhang et.al. [6] and  $20.1\text{ dB}$  better over conventional OFDM system.

#### IV. Conclusion

The proposed F-OFDM system for narrow band IoT devices has been analyzed in this paper by considering the performance parameter ICI, ISI, ACI, PAPR, OoBE and BER for 5-G. The proposed scheme is found  $-5\text{ dB}$  ISI and  $-4.2\text{ dB}$  ICI better than the scheme given by Zhang et.al. It has been identified that ISI shows larger impact on the system than ICI. In our analysis between the filter length and the ACI level has been done and found that the ACI level drops monotonically when the filter length increases. The affect of CP length versus ISI and ICI power are analysed for the F-OFDM system and found the affect on ISI is significant but same time the affect of large CP is not very significant on ICI with large CP length. The proposed filtered OFDM scheme found  $1.6\text{ dB}$  better for large cyclic prefix length. However, for smaller cyclic prefix length overall interference power is not very significant and found comparable. It has been also observed that the performance of F-OFDM is far better in comparison to conventional OFDM power scenario at the transmitter side and at receiver the BER is about  $10^{-6}$  at the SNR of  $45\text{ dB}$ . The proposed filtered-OFDM system for IoT devices used  $7\text{ dB}$  of PAPR whereas the conventional OFDM system takes  $12.1\text{ dB}$  and the scheme given by Zhang et.al. [6] uses  $8.4\text{ dB}$  of PAPR. The proposed F-OFDM system is  $6.5\text{ dB}$  superior in OoBE over the scheme given by Zhang et.al. [6] and  $20.1\text{ dB}$  better over conventional OFDM system. From the conclusion drawn from above observations, we can say that f-OFDM is an excellent candidate for future generations of wireless narrow band IoT systems.

#### Compliance With Ethical Standards

Conflict interests: The authors declare that he has no competing interest.

#### References

- [1]. P. Banelli, S. Buzzi, G. Colavolpe, A. Modenini, F. Rusek, and A. Ugolini, Modulation formats and waveforms for 5G networks: Who will be the heir of OFDM? An overview of alternative modulation schemes for improved spectral efficiency, *IEEE Signal Process. Mag.*, vol. 31, no. 6, pp. 80–93, Nov. 2014.
- [2]. Bogucka H., Kryszkiewicz P., Jiang T., and Kliks A. Dynamic spectrum aggregation for future 5G communications. *IEEE Commun. Mag.*, vol. 53 (5), pp. 35–43, 2015.
- [3]. A. Ijaz et al., "Enabling massive IoT in 5G and beyond systems: PHY radio frame design considerations", *IEEE Access*, vol. 4, pp. 3322-3339, 2016.

- [4]. E. Dahlman, S. Parkvall, J. Skold, 4G: LTE/LTE-Advanced for Mobile Broadband, San Diego, CA, USA: Academic, 2011.
- [5]. Van Eeckhaute, M., Bourdoux, A., De Doncker, P. et al. Performance of emerging multi-carrier waveforms for 5G asynchronous communications. *J Wireless Com Network* 2017, 29 (2017). <https://doi.org/10.1186/s13638-017-0812-8>
- [6]. L. Zhang, A. Ijaz, P. Xiao, M. M. Molu and R. Tafazolli, "Filtered OFDM Systems, Algorithms, and Performance Analysis for 5G and Beyond," in *IEEE Transactions on Communications*, vol. 66, no. 3, pp. 1205-1218, March 2018.
- [7]. X Zhang, L Chen, J Qiu, J Abdoli, On the waveform for 5G. *IEEE Commun. Mag.* 54(11), 74–80 (2016).
- [8]. F. Schaich, T. Wild, "Relaxed synchronization support of universal filtered multi-carrier including autonomous timing advance", *Proc. Int. Symp. Wireless Commun. Syst. (ISWCS)*, pp. 203-208, Aug. 2014.
- [9]. L. Zhang, A. Ijaz, P. Xiao, R. Tafazolli, "Channel equalization and interference analysis for uplink narrowband Internet of Things (NB-IoT)", *IEEE Commun. Lett.*, vol. 21, no. 10, pp. 2206-2209, Oct. 2017.
- [10]. Y. Wang et al., A primer on 3GPP narrowband Internet of Things (NB-IoT), 2016, [online] Available: <https://arxiv.org/abs/1606.04171>.
- [11]. N Michailow, I Gaspar, S Krone, M Lentmaier, G Fettweis, in *International Symposium on Wireless Communication Systems. Generalized frequency division multiplexing: analysis of an alternative multi-carrier technique for next generation cellular systems*, (2012), pp. 171–175.
- [12]. G Fettweis, M Krondorf, S Bittner, in *69th IEEE Vehicular Technology Conference. GFDM - Generalized Frequency Division Multiplexing*, (2009), pp. 1–4.
- [13]. V. Vakilian, T. Wild, F. Schaich, S. ten Brink, J.-F. Frigon, "Universal-filtered multi-carrier technique for wireless systems beyond LTE", *Proc. IEEE Globecom Workshops (GC Wkshps)*, pp. 223-228, Dec. 2013.
- [14]. J. Li, E. Bala, R. Yang, "Resource block filtered-OFDM for future spectrally agile and power efficient systems", *Phys. Commun.*, vol. 11, pp. 36-55, Jun. 2014.
- [15]. X. Yu, Y. Guanghai, Y. Xiao, Y. Zhen, X. Jun, G. Bo, "FB-OFDM: A novel multicarrier scheme for 5G", *Proc. Eur. Conf. Netw. Commun. (EuCNC)*, pp. 271-276, Jun. 2016.
- [16]. D. Chen, X.-G. Xia, T. Jiang, X. Gao, "Properties and power spectral densities of CP based OQAM-OFDM systems", *IEEE Trans. Signal Process.*, vol. 63, no. 14, pp. 3561-3575, Jul. 2015.
- [17]. J. Li, D. Chen, D. Qu, T. Jiang, "Block-wise alamouti schemes for oqam-ofdm systems with complex orthogonality", *Wireless Commun. Mobile Comput.*, vol. 16, no. 17, pp. 2975-2990, Sep. 2016.

Ashutosh Pandey, et. al. "Filtered-OFDM for 5G Wireless Communication Narrow-band IoT Systems." *IOSR Journal of Electrical and Electronics Engineering (IOSR-JEEE)*, 15(3), (2020): pp. 24-31.